# Behavior of trapped ultracold dilute Bose gases at large scattering length near a Feshbach resonance

M. L. Lekala,[1] B. Chakrabarti,[1,*] G. J. Rampho,[1,†] T. K. Das,[2] S. A. Sofianos,[1] and R. M. Adam[3]

[1]*Department of Physics, University of South Africa, P.O. Box 392, Pretoria 0003, South Africa*

[2]*Department of Physics, University of Calcutta, 92 A.P.C. Road, Kolkata 700009, India*

[3]*Nuclear Division, Aveng Africa Limited, 204 Rivonia Road, Morningside 2057, South Africa*

(Received 8 March 2013; revised manuscript received 9 December 2013; published 18 February 2014)

We calculate the ground-state energy and the collective excitation frequency of trapped bosons at large scattering length interacting via the realistic two-body van der Waals potential. Our many-body method keeps two-body correlations produced by all interacting pairs. When the scattering length is small compared to the trap size and the number of bosons in the trap is of the order of a few thousands, the mean-field results are in good agreement with the many-body results. However for large particle numbers, even when the condensate is sufficiently dilute, the interatomic correlation comes into the picture. When the scattering length is quite large near the Feshbach resonance, the Bose gas becomes highly correlated. The many-body results are close to the Gross-Pitaevskii results for a small number of bosons, however, large deviations are noted in the large particle limit. We also calculate the lowest collective excitation and the interaction energy for large scattering lengths. The monopole excitation frequency exhibits a pronounced dependence on the scattering length. We also observe a universal behavior for the interaction energy at the limit of large scattering length.

DOI: 10.1103/PhysRevA.89.023624 PACS number(s): 03.75.Hh, 03.65.Ge, 03.75.Nt

## I. INTRODUCTION

The behavior of Bose-Einstein condensates (BECs) near the Feshbach resonance has been one of the most challenging research areas in the study of ultracold atomic physics [1–7]. In a typical BEC experiment, the average interatomic separation is quite large compared to the range of interatomic interaction [8]. As a result, the study of these dilute inhomogeneous gases were primarily based on the mean-field Gross-Pitaevskii (GP) equation, where the effective mean-field potential is constructed from a contact interaction using the $s$-wave scattering length $a_s$ only [9].

The GP equation is remarkably successful in explaining results from most experiments of gaseous BEC when the gas parameter $na_s^3$ ($n$ is the number density) is very small. However, in recent days there is a new breed of experiments near the Feshbach resonance where a stable BEC is formed at very large scattering lengths, $\sim 10\,000 a_0$ ($a_0$ = Bohr radius), and with a fairly large number of atoms [3–5]. In this parameter regime (large $a_s$) the underlying assumption of the GP equation, such as the shape-independent pseudopotential approximation, disregarding correlations, etc., needs careful scrutiny. The shape-independent approximation (SIA) assumes that the two-body scattering amplitude does not change over the energy range of interest. However, for large $na_s^3$, a larger energy range is involved, requiring consideration of contributions beyond the $s$-wave scattering. Therefore, for large $na_s^3$ the use of SIA becomes questionable. A similar argument is applicable in a strong confinement situation, even at the dilute limit.

In an earlier calculation of Cowell *et al.* [10] for homogeneous systems, it was seen that different potentials having the same scattering length $a_s$ lead to widely varied ground-state energies. The validity of the SIA was first established by Bohn *et al.* [11] only for three trapped bosons which is far from the real experimental situation. It was shown that the SIA is qualitatively good in the low-density limit, however the $\delta$ interaction is not suitable as the correct two-body interaction in the configuration space. The other calculation testing SIA reported in the literature [12] deals with small number of atoms in the condensate and uses the standard short-range two-body potential.

There are some important theories based on the GP equation which go beyond the mean-field GP theory. However, most of the theories are focused on quantum fluctuations [12–15]. In a thorough calculation by Geltman [16], it is pointed out that the replacement of the actual interaction by a contact potential is not appropriate. Giorgini *et al.* [17] also observed the dependence of the ground-state energy on the shape of the two-body potential in the intermediate density regime. The dependency of the ground- and excited-state energies of two- and three-particle condensates on the exact shape of the two-body potential in the high-density limit has also been indicated [12]. In another context Khan and Gao [18] clearly pointed out that the SIA breaks down in the large particle limit in dense condensates.

Near the Feshbach resonance the condensate with a large number of particles becomes highly correlated and is best described by correlated basis functions. Although the earlier study of Blume *et al.* [12] adopted the essentially exact diffusion Monte Carlo (DMC) method, the calculation was restricted to a few hundred atoms only, which is far from the experimental situation. There are also some inspiring theoretical investigations of cold atoms with large scattering length [10,12,19–22]. However, none of these investigations consider real experimental situation, where the long-lived condensate of $10^4$ atoms with scattering length $a_s \simeq 10\,000 a_0$ is produced [3–5]. All the earlier calculations considered from a few tens to a few hundreds of atoms only and the corresponding results already differed significantly from the GP results.

*Permanent address: Department of Physics, University of Kalyani, Nadia, 743215 India.

†ramphogj@gmail.com

 

We use two-body correlated basis functions together with the realistic van der Waals interaction for the description of Bose gases at large scattering lengths near the Feshbach resonance. The two key points of the present study are as follows. We investigate when the effect of interatomic correlation is indeed required, even in the dilute condition ($na_s^3 \ll 1$). We compare our many-body results with the GP and the modified GP equation (MGP), which keeps first order correction in $na_s^3$. Our results clearly show that for the entire range of particle number the many-body energies are in good agreement with both GP and MGP for smaller $a_s$.

After a study of the ground-state properties of dilute Bose gas, we next study repulsive condensate with large scattering length near the Feshbach resonance. In recent-day experiments it is possible to create dilute ($na_s^3 < 1$) but strongly interacting Bose gas near the Feshbach resonance. This type of study is especially important as the effect of interatomic correlation dominates and the zero-range pseudopotential approximation starts to be invalid. For this purpose we choose the scattering length to be 10 and 100 times larger than the natural $^{87}$Rb scattering length and the particle number in the external trap is of the order of a few thousand. Comparison with both GP and MGP results clearly shows that for the large scattering lengths GP fails and MGP results are measurably different from the many-body results. We also observe a universal behavior in the interaction energy of the bosonic system at the large scattering length limit.

Furthermore, the study of the collective excitation frequencies and their dependence on the scattering length will also provide a stringent test to the validity of mean-field approximation and to help judge the beyond-mean-field correction as well as the finite-size effect. Our correlated two-body basis function and the use of the shape-dependent realistic interaction is likely to give rich physics in this respect. Our two-body correlated basis function has been applied recently in the study of dilute Bose gas [23]. The ground-state energies were compared with the GP results for $a_s = 1000a_0$, which is large but away from the recent experimental situation where the long-lived condensate with $10^4$ atoms and $a_s = 10\,000a_0$ at the Feshbach resonance is produced [3–5]. Although our present study uses the same basis functions, the motivation of the this work is completely different. Our earlier work concentrated on the ground-state properties, while our present study considers the collective excitation frequency and shows both the beyond-mean-field and finite-size effects. We also observe a universal behavior of the interacting bosons at such large scattering lengths.

Section II introduces the many-body Schrödinger equation, the correlated basis function, and the many-body effective potential for trapped Bose gases. Results and their interpretation are presented in Sec. III. Section IV presents conclusions.

## II. MANY-BODY CALCULATION

### A. Potential harmonics expansion method

The many-body Schrödinger equation for a condensate having $N$ identical bosons, each having mass $m$, in a spherical trap with trap frequency $\omega_{\rm ho}$ is given by

$$\sum_{i=1}^{N}\left[-\frac{\hbar^2}{2m}\nabla_i^2+\frac{m}{2}\omega_{\rm ho}^2 r_i^2+\sum_{j>i}^{N}V(\vec{r}_{ij})\right]\Psi = E\Psi. \quad (1)$$

In this equation $V(\vec{r}_{ij})$ is the interaction potential where $\vec{r}_{ij} = \vec{r}_i - \vec{r}_j$ with $\vec{r}_i$ being the position vector of the $i$th boson, $\omega_{\rm ho}$ is the frequency of external trap, and $E$ is the total energy of the system. Next we introduce a set of $\mathcal{N} = N-1$ Jacobi vectors $(\vec{\zeta}_i, i = 1,\ldots,\mathcal{N})$, then the relative motion of the bosons is described by [24]

$$\left[-\frac{\hbar^2}{m}\sum_{i=1}^{\mathcal{N}}\nabla_{\zeta_i}^2 + V_{\rm trap} + V_{\rm int}(\vec{\zeta}_1,\ldots,\vec{\zeta}_{\mathcal{N}}) - E_R\right] \times \Psi(\vec{\zeta}_1,\ldots,\vec{\zeta}_{\mathcal{N}}) = 0, \quad (2)$$

where $V_{\rm int}$ is the sum of all pairwise interaction and $E_R$ the internal energy of the system, with $E = E_R + \frac{3}{2}\hbar\omega_{\rm ho}$.

The hyperspherical harmonic expansion method (HHEM) is an *ab initio* tool to solve the many-body Schrödinger equation where the total many-body wave function is expanded in the complete set of hyperspherical harmonics (HH) basis which retains *all many-body* correlations [25]. However, due to the large degeneracy of HH basis, it cannot be applied to BEC which contains few thousands to few millions of atoms. To simplify calculations greatly, we introduce instead the basis functions of the potential harmonics (PH) [26], which retain *only the two-body* correlations. Such basis functions are manifestly justified for the dilute BECs, where interparticle separations are much larger than the interaction range. This approach can be easily extended to the limit of large particle number.

The physical meaning of the PH basis is when the $(ij)$ pair interacts, all remaining particles are noninteracting spectators. This picture is true for all possible $(ij)$ pairs. Thus we choose $\vec{\zeta}_{\mathcal{N}}$ as the $\vec{r}_{ij}$ for the interacting $(ij)$ pair and the remaining Jacobi vectors are used to define the hyperradius of $(N-2)$ noninteracting particles as $\rho_{ij}^2 = \sum_{i=1}^{\mathcal{N}-1}\zeta_i^2$, so that $r^2 = \rho_{ij}^2 + r_{ij}^2$, where $r$ is called the global hyperradius and it defines the average size of the condensate in the hyspherical space. The hyperangle $\phi$ is introduced such that $r_{ij} = r\cos\phi$ and $\rho_{ij} = r\sin\phi$. This permits us to decompose the total wave function $\psi$ into a two-body Faddeev component for the interacting $(ij)$ pair [24],

$$\Psi = \sum_{i,j>i}^{N}\phi_{ij}(\vec{r}_{ij}, r). \quad (3)$$

Note that the Faddeev component $\phi_{ij}$ is a function of the two-body separation vector $\vec{r}_{ij}$ and the global length $r$ only, since all the noninteracting particles are simply spectators. Thus, the effect of two-body correlation comes through the two-body interaction in the expansion basis. Again as the noninteracting particles are simply spectators, the angular and hyperangular momentum of the system are contributed by the interacting pair only.

The two-body Faddeev component is next expanded in the potential harmonics (PH) basis $\{\mathcal{P}^{\ell m}_{2K+\ell}(\Omega^{ij}_{\mathcal{N}})\}$ [24,27,28],

$$\phi_{ij}(r_{ij}) = \frac{1}{r^{(3\mathcal{N}-1)/2}} \sum_K \mathcal{P}^{\ell m}_{2K+\ell}\big(\Omega^{ij}_{\mathcal{N}}\big) u^{\ell}_K(r). \tag{4}$$

The PH basis is a subset of the full HH basis that is sufficient for the expansion of the potential $V(\vec{r}_{ij})$. Hence $\{\mathcal{P}^{\ell m}_{2K+\ell}(\Omega^{ij}_{\mathcal{N}})\}$ depends only on $\vec{r}_{ij}$ and $r$. It is independent of the remaining Jacobi vectors. Substitution of this in the Faddeev equation and projection with the PH for the $(ij)$ partition gives a set of coupled differential equation (CDEs) [24,27,28],

$$\left\{\frac{\hbar^2}{m}\left[-\frac{d^2}{dr^2} + \frac{\mathcal{L}(\mathcal{L}+1)+4K(K+\kappa)}{r^2}\right] + V_{\rm trap}(r)\right\} U_{K\ell}(r) + \sum_{K'} f_{K\ell} V_{KK'}(r) f_{K'\ell} U_{K'\ell}(r) = E_R\, U_{K\ell}(r), \tag{5}$$

where $\kappa = \alpha+\beta+1$, $\mathcal{L} = \ell + (3N-6)/2$, $U_{K\ell}(r) = f_{K\ell} u^{\ell}_K(r)$, $\alpha = (3N-8)/2$, and $\beta = \ell + 1/2$. $f^2_{K\ell}$ is a constant and represents the overlap of the PH for interacting partition with the sum of PHs corresponding to all partitions [26]. $V_{KK'}(r)$ is the potential matrix element [24]. One can in principle solve Eq. (5) exactly or by adiabatic approximation to obtain the energy and wave function of the condensate.

### B. Introduction of short-range correlation

In the laboratory BECs at temperatures $\sim$100 nK, the energy of the interacting pair is negligibly small ($\sim 10^{-13}$ eV) compared to the energy scale of interatomic interaction ($\sim$1 eV). Therefore, the effective two-body interaction is characterized by the zero-energy scattering length $a_s$ (which is typically $\sim 100a_0$–$1000a_0$). However, a realistic interatomic interaction is always attractive at large separations (greater than $10a_0$) with a short-range ($\sim 10a_0$) repulsive hard core. In order that $\phi_{ij}$ reflects the effect of this strong repulsion between the $(ij)$ pair of bosons at short separations, we introduce an additional short-range correlation function. Without the correlation function the convergence of the above expansion [Eq. (4)] is very slow as the pair of particles with practically zero kinetic energy do not come closer than $\simeq |a_s|$. However, the zeroth-order PH is a constant [24] and would give a large probability even for $r_{ij} \to 0$. Therefore, we multiply the PH basis with the additional correlation function $\eta(r_{ij})$ which has the same short-separation behavior as $\phi_{ij}(\vec{r}_{ij}, r)$. Thus, the short-separation behavior of $\phi_{ij}(\vec{r}_{ij}, r)$ is given by the zero-energy solution $\eta(r_{ij})$ of the $(ij)$ pair interacting through $V(r_{ij})$,

$$\left[-\frac{\hbar^2}{m}\frac{1}{r^2_{ij}}\frac{d}{dr_{ij}}\left(r^2_{ij}\frac{d}{dr_{ij}}\right) + V(r_{ij})\right]\eta(r_{ij}) = 0. \tag{6}$$

Its asymptotic form quickly attains $\eta(r_{ij}) \sim C(1 - a_s/r_{ij})$, from which $a_s$ is obtained [29].

The new basis including $\eta(r_{ij})$ is referred to as the correlated PH (CPH) basis and we replace Eq. (4) by

$$\phi_{ij}(\vec{r}_{ij}, r) = \frac{1}{r^{(3\mathcal{N}-1)/2}} \sum_K \mathcal{P}^{\ell m}_{2K+\ell}\big(\Omega^{ij}_{\mathcal{N}}\big) u^{\ell}_K(r)\eta(r_{ij}). \tag{7}$$

The corresponding correlated potential matrix element is given by

$$V_{KK'}(r) = \frac{1}{\big(h^{\alpha\beta}_K h^{\alpha\beta}_{K'}\big)^{\frac{1}{2}}} \int_{-1}^{+1} P^{\alpha\beta}_K(z) V\big(r\sqrt{(1+z)/2}\big) \times P^{\alpha\beta}_{K'}(z)\eta\big(r\sqrt{(1+z)/2}\big) W_\ell(z)\, dz. \tag{8}$$

Here $P^{\alpha\beta}_K(z)$ are the Jacobi polynomials and their norm is $h^{\alpha\beta}_K$ and weight function is $W_\ell(z)$. The inclusion of $\eta(r_{ij})$ in the PH basis dramatically enhances the rate of convergence of the expansion, however, it also makes the expansion basis nonorthogonal. Standard procedure can handle this, but the process becomes quite involved and slow in the numerical procedure. Actual calculation shows that $\eta(r_{ij})$ is different from a constant only in a very narrow interval ($\sim 50a_0$) near the origin. This makes the overlap matrix close to a constant matrix. Its effect is then approximately taken through the empirically obtained asymptotic constant $C$.

### C. Solution of the CDE

Even though the CDE Eq. (5) with the correlated potential matrix [Eq. (7)] can be solved exactly by the renormalized Numerov method, we choose to use the hyperspherical adiabatic approximation (HAA) [30]. Besides being much faster than the exact numerical method, the HAA generates an *effective potential* in the hyperradial space, providing a clear physical picture of the collective motion. In HAA, we assume that the hyperradial motion is slow compared to the hyperangular motion. This is justified, since the hyperradial motion corresponds to the breathing mode of the system and is very slow in the externally applied low-frequency trap compared to other modes of the many-body system. The hyperangular motion is thus decoupled adiabatically (as in the Born-Oppenheimer approximation) and solved for a fixed value of hyperradius $r$. The latter is achieved by diagonalizing the potential matrix together with the hypercentrifugal repulsion for a fixed value of $r$.

The lowest eigenvalue $\omega_0(r)$ (as a parametric function of $r$) provides the effective potential for the hyperradial motion. Thus $\omega_0(r)$ is the effective potential in which the condensate moves collectively. The energy and wave function of the condensate are finally obtained by solving the adiabatically separated hyperradial equation in the extreme adiabatic approximation (EAA),

$$\left[-\frac{\hbar^2}{m}\frac{d^2}{dr^2} + \omega_0(r) - E_R\right]\zeta_0(r) = 0, \tag{9}$$

subject to appropriate boundary conditions on $\zeta_0(r)$. For our numerical calculation we fix $\ell = 0$ and truncate the CPH basis to a maximum value $K = K_{\rm max}$ requiring proper convergence. For our present calculation convergence is attained at $K_{\rm max} = 4$.

The advantage of the above correlated potential harmonic expansion method (CPHEM) is that the correlated two-body basis function takes care of both the short- and long-range correlations and keeps only *four* variables for all $N$ (remaining irrelevant degrees of freedom in the dilute condensate being frozen out), which drastically reduces the numerical

difficulties. Furthermore, in contrast with a shape-independent zero-range potential in the GP equation, one may use any realistic finite range potential in the CPHEM. The effective two-body potential for the condensate, starting from any realistic interatomic potential $V(r_{ij})$, has to have *the correct long-range behavior in terms of* $a_s$. This is assured through the introduction of $\eta(r_{ij})$ in Eq. (8) [28]. For example, the van der Waals potential, with a hard-core repulsion and an attractive long tail, provides a realistic picture, which is particularly relevant in the limit of large scattering length. For $a_s = 10\,000a_0$ and $N = 2000$, the interparticle separation is comparable with the range ($|a_s|$) of the *effective two-body interaction for the condensate*. The present technique produces this effective interaction, having the correct tail of the realistic potential corresponding to the appropriate $a_s$. Moreover, this approach further reduces the $3(N-1)$-dimensional problem to an effectively one-dimensional problem in the adiabatic approximation, for which the resultant many-body effective potential provides all the qualitative and quantitative features.

## III. RESULTS AND DISCUSSION

### A. Choice of interaction

The system parameters are the mass $m = m(^{87}\text{Rb})$ and frequency $\omega_{\text{ho}} = 2\pi \times 77.78$ Hz, corresponding to the JILA trap. The trap length $a_{\text{ho}} = \sqrt{\hbar/m\omega_{\text{ho}}}$ is chosen as the unit of length and harmonic oscillator energy $\hbar\omega_{\text{ho}}$ is taken as the unit of energy. These are referred to as the oscillator units (o.u.) of length and energy respectively. For the mean-field GP equation the two-body potential chosen is the zero-range potential $V(r) = (4\pi\hbar^2 a_s/m)\,\delta(r)$. It is assumed that the single parameter $a_s$ provides the correct zero-energy scattering amplitude. From the two-body scattering, the zero-range potential given above correctly gives the scattering amplitude at zero range in the first Born approximation. It is shape independent as it ignores completely the energy dependence of the scattering amplitude. It is a good approximation when $na_s^3$ is small.

We choose the realistic van der Waals potential

$$V(r_{ij}) = \begin{cases} -C_6/r_{ij}^6 & \text{for} \quad r_{ij} > r_c, \\ \infty & \text{for} \quad r_{ij} \leqslant r_c \end{cases} \tag{10}$$

with $C_6 = 6.489\,755 \times 10^{-11}$ o.u. for $^{87}$Rb atoms. This interaction potential is justified for the description of the experimentally achieved condensate [29]. For a given value of $r_c$, $a_s$ can be calculated analytically solving Eq. (6) for the van der Waals potential given by Eq. (10) or equivalently Eq. (5.43) of Ref. [29]. We choose the $r_c$ value which corresponds to the single-node in the two-body wave function. The value of $r_c$ is $1.121\,054 \times 10^{-3}$ o.u. which corresponds to $a_s = 0.004\,33$ o.u. and mimics the JILA trap experiment. The relation of the scattering length to the effective range is briefly discussed in Appendix A.

### B. Dilute BEC ($na_s^3 \ll 1$)

To facilitate discussions we point out that in a laboratory BEC there are three very different length scales: the trap length $a_{\text{ho}} = \sqrt{\hbar/(m\omega_{\text{ho}})} \sim 2.3 \times 10^4 a_0$, the scattering length $a_s = 100a_0$ which is the range of effective interaction of nearly zero-energy bosons, and the range of actual two-body interatomic interaction $r_{2B}$ ($\sim 65a_0$ for van der Waals potential for Rb atoms). The indicated values of $a_s$ and $a_{\text{ho}}$ correspond to the original JILA experiment for Rb atoms. For $N$ bosons in the trap the number density is $n \sim N/a_{\text{ho}}^3$, with average interparticle separation $\sim a_{\text{ho}}/N^{1/3}$. We then define two different types of diluteness: (1) A condensate is "physically dilute" when average interparticle separation is large compared to $r_{2B}$, i.e., $r_{2B}N^{1/3}/a_{\text{ho}} \ll 1$. (2) A condensate is dilute in "gas parameter" when $n|a_s|^3 \ll 1$. When a condensate is not physically dilute, the atoms "see" the details of the actual interatomic interaction. On the other hand, when a condensate is physically dilute but dense in gas parameter, atoms interact only through zero-energy effective interaction in terms of $a_s$, but correlations become more relevant.

We first study the ground state of a system of $^{87}$Rb atoms in an isotropic harmonic trap with the chosen parameter as given earlier. The natural $s$-wave triplet scattering length for $^{87}$Rb is $a_s = 100a_0$. Therefore, the gas parameter is $na_s^3 < 8.1 \times 10^{-3}$ for $N < 10^5$, which satisfies the criterion of diluteness. We fix the scattering length and vary the number of bosons from very few to quite a large number. We compare our many-body results with the widely used mean-field GP approach. The relevant equations of this GP approach are indicated in Appendix B.

In Fig. 1 we plot the ground-state energy per particle as a function of $\log_{10}(N)$. There is almost no noticeable difference between many-body results and the mean-field results when the number of bosons in the trap is of the order of a few thousands. For much higher $N$ the GP results are slightly smaller than the many-body results. As the MGP equation partly incorporates two-body physics, the MGP results are closer to our many-body results. However a small difference between the MGP and CPHEM exists which is attributed to the use of shape-dependent potential and all two-body correlations in the many-body calculation. Thus we do not observe any significant deviation between the mean-field and the many-body results in the dilute gas parameter situation.

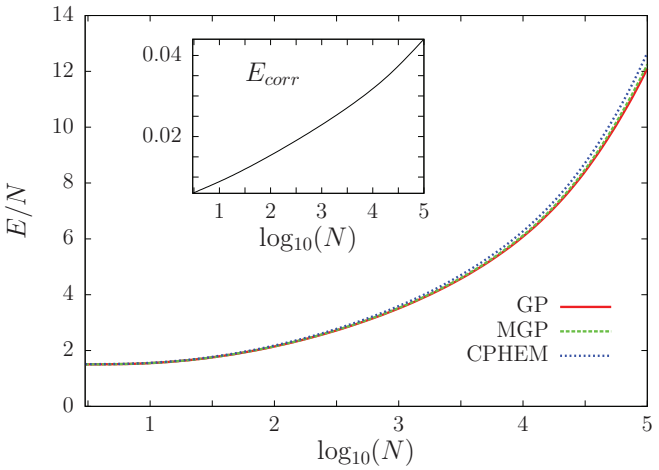


FIG. 1. (Color online) Ground-state energy per atom (in o.u.) as a function of $\log_{10}(N)$ for scattering length ($a_s = 100a_0$) obtained by the CPHEM. The GP results are obtained by solving Eq. (B1) and the MGP results are obtained by solving Eq. (B2). The normalized correlation energy [Eq. (11)]. is shown in the inset.

It is seen from Fig. 1 that our many-body energies are always equal to or larger than the mean-field energies. We, therefore, define the energy difference $E_{\rm CPHEM} - E_{\rm GP}$ as the correlation energy. We plot the normalized correlation energy

$$E_{\rm corr} = \frac{E_{\rm CPHEM} - E_{\rm GP}}{E_{\rm CPHEM}} \tag{11}$$

as a function of $\log_{10}(N)$ in Fig. 1 (inset). The correlation energy is quite small as the system is extremely dilute, however it smoothly increases with $N$. It indicates that the effect of correlation will be significant at large scattering lengths.

We are using a realistic and shape-dependent potential. The validity of SIA is questionable whenever the interparticle separation is comparable to the range of two-body realistic interaction, even though the condensate is extremely dilute in the gas parameter. This can be investigated by increasing the range of the two-body realistic interaction by increasing $C_6$, while keeping $a_s$ constant. We feel that the present work is a good platform to check the validity of SIA in this way. Thus we vary $C_6$, making it larger than the corresponding experimental value and observe how the condensate properties are affected by the strength of the long-range tail of the two-body potential. The two additional values of $C_6$ which we choose are $10 \times 10^{-11}$ and $50 \times 10^{-11}$ o.u. For each value of $C_6$, we calculate the corresponding $r_c$ such that $a_s$ has the same value. For each set of $(C_6, r_c)$, we solve the many-body equation for $N = 10, 100, 1000, 10\,000$ bosons, and the results are given in Table I.

It can be seen from this table that as $C_6$ increases the potential becomes more attractive, but simultaneously $r_c$ also increases, although by a small amount. Therefore, the net two-body attraction calculated from the volume integral $4\pi \int_{r_c}^{\infty} V(r) r^2 dr$ increases. Note that this change occurs in each two-body pair which goes as $N(N-1)/2$ while the trap energy and the kinetic energy increases as $N$. For smaller $N$, these two nearly balance. Thus, the effect of increasing $C_6$ on the ground-state energy of the condensate is negligible for small $N$ and SIA is well obeyed. However for larger $N$, the net contribution from all pairs becomes appreciably negative which causes a decrease in the total energy. Although the condensate energy is grossly well reproduced by the mean-field theory in the dilute condition, the dependence of the ground-state energy on the shape of the two-body potential in the large particle-number limit definitely points to the need for the use of a realistic interaction, especially for large scattering lengths when the condensate becomes more correlated.

TABLE I. Ground-state energy per particle (in o.u.) for different $C_6$ parameters. The different ($C_6$ and $r_c$) combination produces the same scattering length $a_s = 100\,a_0$. For comparison the GP results are also presented. $C_6$, $r_c$ and energy values are in o.u.

| $C_6$ (o.u.) | $6.489 \times 10^{-11}$ | $10 \times 10^{-11}$ | $50 \times 10^{-11}$ |
|---|---|---|---|
| $r_c$ (o.u.) | $1.121 \times 10^{-3}$ | $1.237 \times 10^{-3}$ | $1.761 \times 10^{-3}$ |
| $N$ | 10 | 10 | 10 |
| $(E/N)_{\rm CPHEM}$ | 1.522 | 1.522 | 1.522 |
| $(E/N)_{\rm GP}$ | 1.515 | 1.515 | 1.515 |
| $N$ | 100 | 100 | 100 |
| $(E/N)_{\rm CPHEM}$ | 1.677 | 1.676 | 1.674 |
| $(E/N)_{\rm GP}$ | 1.651 | 1.651 | 1.651 |
| $N$ | 1000 | 1000 | 1000 |
| $(E/N)_{\rm CPHEM}$ | 2.434 | 2.427 | 2.419 |
| $(E/N)_{\rm GP}$ | 2.424 | 2.424 | 2.424 |
| $N$ | 10000 | 10000 | 10000 |
| $(E/N)_{\rm CPHEM}$ | 5.198 | 5.178 | 5.155 |
| $(E/N)_{\rm GP}$ | 5.043 | 5.043 | 5.043 |

TABLE II. CPHEM ground-state energy per particle (in o.u.) using a van der Waals and $\delta$ (CPHEM$_\delta$) interactions with $a_s = 100 a_0$. GP with contact $\delta$ interaction and DMC with hard-core interaction [12] are also presented. Column 2 determines the diluteness of the condensate.

| $N$ | $na_s^3$ | CPHEM | CPHEM$_\delta$ | DMC | GP |
|---|---|---|---|---|---|
| 3 | $10^{-7}$ | 1.512 | 1.502 | 1.503 | 1.503 |
| 5 | $10^{-7}$ | 1.519 | 1.506 | 1.507 | 1.507 |
| 10 | $10^{-6}$ | 1.523 | 1.514 | 1.515 | 1.515 |
| 20 | $10^{-6}$ | 1.548 | 1.531 | 1.532 | 1.532 |
| 100 | $10^{-5}$ | 1.677 | 1.652 | 1.651 | 1.651 |
| 1000 | $10^{-4}$ | 2.434 | 2.477 | | 2.424 |

We also calculate ground-state energies using the many-body approach with the contact interaction. We replace $V(\vec{r}_i - \vec{r}_j)$ term in the Schrödinger equation by $V(\vec{r}_i - \vec{r}_j) = (4\pi\hbar^2 a_s/m)\,\delta(\vec{r}_i - \vec{r}_j)$ and solve the coupled equation as before. The results are presented in Table II for up to 1000 bosons, where the condition for true diluteness is well satisfied. In the same table, we also present the DMC results for hard-core bosons [12] and GP results. It is nicely seen that in very dilute condition all results are basically indistinguishable. However for $N = 1000$, although the system is quite dilute in the gas parameter, the result for van der Waals interaction is below the result of $\delta$ interaction. This is in perfect agreement with our previous observation that the effect of shape-dependent potential really comes into the picture for larger $N$.

### C. Large scattering length

In the next part of our work we consider the Bose gas near Feshbach resonance. In Table III, we present the ground-state energy per atom, in units of $\hbar\omega_{\rm ho}$, for $a_s = 1000 a_0$

TABLE III. CPHEM ground-state energy per particle (in o.u.) for $N = 3$–$20$ $^{87}$Rb atoms in the isotropic trap using the van der Waals and $\delta$ (CPHEM$_\delta$) interactions for $a_s = 1000 a_0$ (top) and $a_s = 10\,000 a_0$ (bottom). The GP and MGP results are also presented for comparison.

| $N$ | $na_s^3$ | CPHEM | CPHEM$_\delta$ | GP | MGP |
|---|---|---|---|---|---|
| 3 | $10^{-4}$ | 1.549 | 1.525 | 1.533 | 1.534 |
| 5 | $10^{-4}$ | 1.595 | 1.555 | 1.565 | 1.566 |
| 10 | $10^{-3}$ | 1.713 | 1.628 | 1.638 | 1.642 |
| 20 | $10^{-3}$ | 1.890 | 1.759 | 1.764 | 1.774 |
| 3 | 0.243 | 1.794 | 1.685 | 1.776 | 1.870 |
| 5 | 0.405 | 2.024 | 1.895 | 1.980 | 2.154 |
| 10 | 0.811 | 2.512 | 2.307 | 2.361 | 2.684 |
| 20 | 1.623 | 3.074 | 2.903 | 2.895 | 3.425 |

and $a_s = 10\,000a_0$ for a smaller number of particles. The condensate is purely dilute in the former case, while it is physically dilute but fairly dense in the gas parameter in the latter case. We observe that for $a_s = 1000a_0$, the MGP results, which are considered in the literature as better than the GP results, are closer to the many-body energies. However for $a_s = 10\,000a_0$, the many-body energies are consistently lower than the MGP results. The consistently smaller value in the many-body ground-state energy signifies the effect of *long-range* correlation due to the presence of an attractive van der Waals tail in the realistic potential, when the condensate becomes highly correlated at large pair separation. It also signifies that MGP takes into account the correct two-body physics, however additional shape-dependent correction is indeed required.

For a closer comparison with the GP which uses the contact interaction, we repeat our many-body calculation with the contact interaction and present our results in the fourth column of Table III. It can be seen that the CPHEM energies for the contact interaction are consistently smaller than GP energies. For larger $N$ and intermediate ($a_s = 1000a_0$) and large ($a_s = 10\,000a_0$) scattering length, we plot the interaction energy per atom ($E/N - 1.5$) as a function of the number of bosons $N$ in Fig. 2 for the GP, MGP, and the many-body CPHEM. For intermediate scattering length and moderate atom number, although the system is dilute ($na_s^3 < 1$), interatomic correlation strongly dominates. From lower part of Fig. 2, we see that there is very little difference between CPHEM and MGP results which nicely demonstrate that for such density regime, only the two-body correlation is effective.

For large scattering length the condensate becomes strongly correlated, and the mean-field results for GP and MGP differ by large amounts. The mean-field approximation is no longer accurate. The GP energy is consistently lower than the many-body results whereas MGP energy overshoots the CPHEM ground-state energy. This observation is also in perfect agreement with Table III, where even for very small values of $N$, MGP results overshoot the many-body results. The MGP functional yields energies which are too high as $N$ becomes larger. It is due to the fact that the MGP energy functional keeps the two-body physics but ignores the shape-dependent correction term. The attractive van der Waals tail, that must appear in *every* realistic two-body potential, lowers the ground-state energy. It becomes important when the range of the effective two-body interaction $|a_s|$ becomes large. Therefore, an additional shape-dependent correction term in the MGP functional may improve the situation. At the same time the two-body basis function may also be inadequate to describe such a strongly correlated system as beyond-two-body correlation may become important. This would be an interesting issue for future study. It should be noted that using our method we can obtain results for $N > 2000$, but mean-field results using the program of Ref. [31] become unstable above this limit.

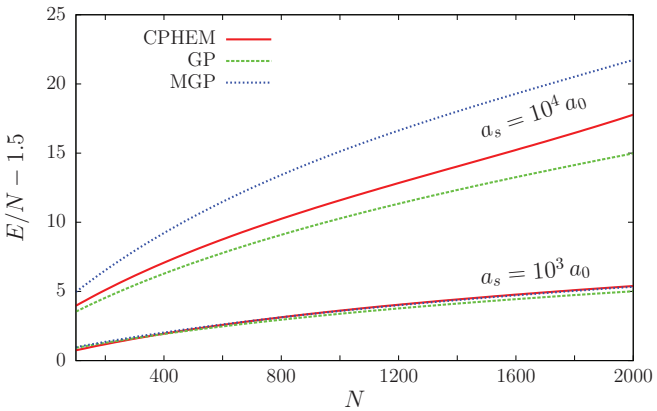


FIG. 2. (Color online) Interaction energy per atom (in o.u.) as a function of the number of bosons in the condensate of $^{87}$Rb for intermediate scattering length ($a_s = 10^3 a_0$: bottom panel) and for large scattering length ($a_s = 10^4 a_0$: upper panel), obtained by the CPHEM. The GP results are obtained by solving Eq. (B1) and the MGP results are obtained by solving Eq. (B2).

### D. Excitation frequencies

We also calculate excitation frequencies to observe both the finite-size effect and the beyond-mean-field effect. The study of the frequencies of collective oscillations of a trapped Bose gas, interacting with large scattering length, is also important as it provides an excellent confirmation of the prediction of mean-field theory. The positive atomic scattering length close to the Feshbach resonance is associated with the occurrence of a weakly bound molecular state. In the low-density limit one may expect the formation of Bose-Einstein condensation of molecules which is described by the GP theory. Typically when the gas parameter $na_s^3 \ll 1$, i.e., the average distance between particles is significantly larger than the range of the effective two-body potential, the mean-field prediction is quite accurate. In the Thomas-Fermi (TF) limit of large particle number in an isotropic trap, the frequencies of collective oscillation obey the dispersion relation [9]

$$\omega(n_r,\ell) = \omega_{\rm ho}\left(2n_r^2 + 2n_r\ell + 3n_r + \ell\right)^{1/2}, \qquad (12)$$

where $n_r$ is the number of radial nodes and $\ell$ is the angular momentum of excitation. It shows that the collective frequencies in the mean-field theory are fixed. The effect of going beyond the mean-field theory was studied by Pitaevskii and Stringari [32]. For the large $N$ limit the first correction to the collective frequencies due to some beyond-mean-field effects was provided by an analytic calculation [32].

The lowest mode in a spherical trap is the breathing mode which is characterized by $n_r = 1$ and $\ell = 0$. The fractional shift in the monopole frequency ($\omega_M$) is given by

$$\frac{\delta\omega_M}{\omega_M} = \frac{63\sqrt{\pi}}{128}\sqrt{n(0)a_s^3}, \qquad (13)$$

where $n(0)$ is the density at the center of the trap and the gas parameter can be written as

$$n(0)a_s^3 = \frac{15^{2/5}}{8\pi}\left(\frac{N^{1/6}a_s}{a_{\rm ho}}\right)^{12/5}. \qquad (14)$$

This fractional shift is insignificant for low-density, even for large $N$. However, it may be significant for large $a_s$ limit. Thus, the many-body investigation in this direction, measuring the correlation effect beyond the mean-field, is challenging.

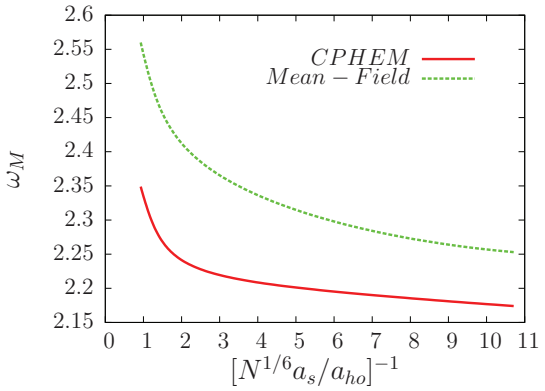


FIG. 3. (Color online) Monopole frequency (in units of $\omega_{\rm ho}$) close to the Feshbach resonance as a function of the dimensionless parameter $(N^{1/6}a_s/a_{\rm ho})^{-1}$. The mean-field graph corresponds to the dispersion relation Eq. (11) accounting for the beyond-mean-field correction Eq. (13).

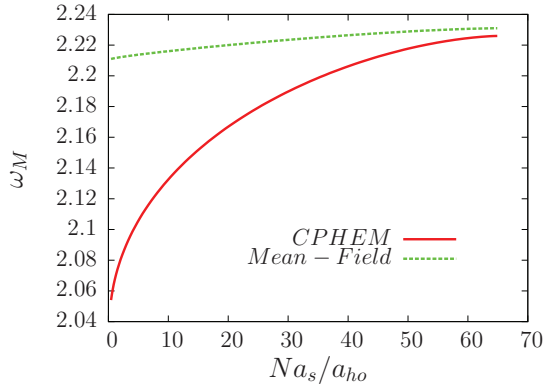


FIG. 4. (Color online) Monopole frequency (in units of $\omega_{\rm ho}$) as a function of $Na_s/a_{\rm ho}$ for a finite number of atoms in the low-density regime. The mean-field result takes into account the finite-size effect Eq. (11) together with Eq. (15).

As pointed out earlier, in HAA the coupling potential matrix together with the diagonal hypercentrifugal repulsion (for a fixed $r$) is diagonalized to get the effective potential $\omega_0(r)$, which is the lowest eigenpotential of the potential matrix, as a parametric function of $r$. In this picture, the whole condensate exhibits collective motion in the effective potential $\omega_0(r)$. The energy levels $E_{n\ell}$ of the system are calculated as excitations in the effective potential for orbital angular momentum $\ell$ of the system. Thus the ground-state energy of the condensate ($E_{00}$) in this well corresponds to $n = 0$, $\ell = 0$, whereas $E_{n\ell}$ is the $n$th radial excitations of the $\ell$th surface mode. The lowest hyperradial excitation corresponding to the breathing mode for $\ell = 0$ gives the monopole frequency as $\omega_M = (E_{10} - E_{00})/\hbar$.

As the beyond-mean-field correction depends on the combination $N^{1/6}a_s/a_{\rm ho}$, in Fig. 3 we plot the monopole frequency as a function of $[N^{1/6}a_s/a_{\rm ho}]^{-1}$. Although the many-body and the mean-field graphs describe the beyond mean-field effect correctly, the extrapolation to the asymptotic region of the noninteracting Bose gas for larger argument reveals appreciable deviations. This is because the mean-field result takes the TF limit with a very large particle number, whereas our many-body calculation takes a finite number of atoms. Thus an additional correction term in the monopole frequency due to the finite-size effect is needed to describe the present day experiment. The finite-size effect arises as the mean-field prediction of monopole frequency ($\simeq\sqrt{5}\omega_{\rm ho}$) holds only in the large-$N$ limit where the quantum pressure term is ignored.

Using a sum-rule approach, Pitaevskii and Stringari proposed a leading-order correction to the monopole frequency in the large particle limit as [32]

$$\frac{\delta\omega_M}{\omega_M} = -\frac{7}{6}\left(\frac{a_{\rm ho}}{R}\right)^4 \log_{10}\left(\frac{R}{Ca_{\rm ho}}\right), \qquad (15)$$

where $R = a_{\rm ho}(15Na_s/a_{\rm ho})^{1/5}$ and $C = 1.3$. In the large particle number limit this finite-size shift will vanish but it is important for a small particle number even in the dilute regime. Therefore, for our present many-body calculation, we consider the effect of both the beyond-mean-field and finite size. As the finite-size effect depends on $Na_s/a_{\rm ho}$, in Fig. 4 we plot the monopole frequency as a function of $Na_s/a_{\rm ho}$. Comparing with Fig. 3 we find that the finite-size shift of the monopole oscillation is much smaller than the beyond-mean-field effect correction.

Another important issue is the behavior of the ground-state energy in the large scattering length limit. In Figs. 5 and 6 we plot the interaction energy per particle by CPHEM as a function of $Na_s/a_{\rm ho}$ (using a logarithmic scale) for different particle numbers. It is seen that the many-body results for $N = 100$ and $N = 1000$ are separated in Fig. 5, for smaller values of $Na_s/a_{\rm ho}$ corresponding to $a_s$ up to $1000a_0$. This implies that the system does not show a universal behavior as the many-body effect dominates. However, for large scattering length comparable to the trap size, we observe in Fig. 6 that the many-body results for $N = 1000$ and $N = 10\,000$ absolutely overlap, which clearly exhibits a universal behavior indicating that our many-body treatment may be directly extrapolated for larger $N$ and $a_s$. We can understand the universal behavior in the following manner. Since $a_s$ is the effective range of interaction, for $a_s \ll a_{\rm ho}$, not all pairs in the condensate interact. For a fixed value of $Na_s/a_{\rm ho}$, as $N$ increases, both $a_s$ and the average interparticle separation (which is $\sim a_{\rm ho}/N^{1/3}$)

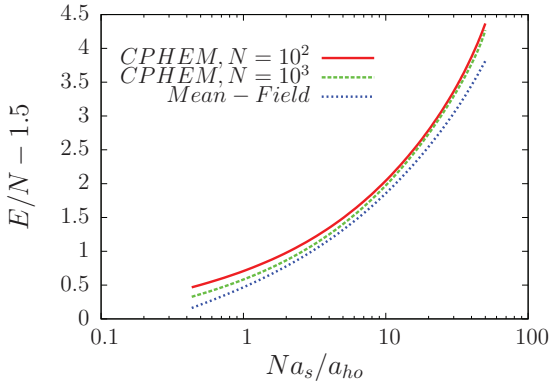


FIG. 5. (Color online) (a) Interaction energy per atom (in o.u.) by CPHEM as a function of $Na_s/a_{\rm ho}$ for $N$ identical bosons in the trap. Note the logarithmic scale. The zero-range GP results are also shown.

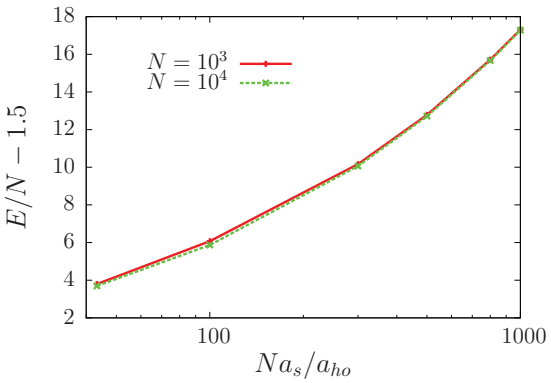


FIG. 6. (Color online) Same as in Fig. 5 for large values of $Na_s/a_{ho}$ near the Feshbach resonance. All data points for $N = 1000$ and $N = 10\,000$ line up on a universal curve.

decrease; but they decrease differently, and the number of *interacting pairs* depends on $N$. Hence energy per particle depends on $N$, for the same value of $Na_s/a_{ho}$. But when $a_s$ is comparable to or greater than $a_{ho}$, all pairs interact. Hence energy per particle becomes independent of $N$ for the same value of $Na_s/a_{ho}$, resulting in a universal behavior.

Before closing the discussion it is also necessary to observe when the effect of three-body correlation will come into the picture. In the strong interacting regime the two-body correlation is still dominating, however the effect of three-body correlations also builds up with increase in $na_s^3$. Thus it is indeed required to calculate the loss of atoms per second due to three-body recombination. The three-body loss rate for $N$-atom condensate is defined as

$$\Gamma_N = LN^3 \int d^3\vec{x}[\phi(\vec{x})]^6, \tag{16}$$

where $\phi(\vec{x})$ is the condensate wave function. For $^{87}$Rb atoms the three-body recombination coefficient is $L = 4.0 \times 10^{-30}$ cm$^6$/s [29]. In CPHEM, the wave function $\psi$ is initially obtained as a function of the Jacobi coordinates. It is then transformed into a function of position vectors $[\vec{x}_1, \vec{x}_2, \ldots \vec{x}_N]$. Finally the one-body density is used for $|\phi(x)|^2$ to calculate $\Gamma_N$.

In Fig. 7, we present the values of $\Gamma_N$ as a function of $N$ for $a_s = 1000a_0$ and $a_s = 10\,000a_0$ and maximum number of bosons $N = 2000$ as before. It is seen that for small values of $N$ the loss of atoms per second due to three-body recombination is negligible for both choices of the scattering length. For a fixed $a_s$, the value of $\Gamma_N$ smoothly increases with $N$ as expected. However for a fixed $N$, but larger $a_s$, the value of $\Gamma_N$ decreases, as increasing $a_s$ means the system becomes more repulsive and the condensate density $|\phi(x)|^2$ becomes more spread out towards the boundary of the trap. This causes a decrease in $\Gamma_N$, as the probability of three particles coming close together reduces due to the lower density. However this pattern will be continued until the condensate density fills the trap size. After that we will enter in the strongly interacting dense regime where one may expect sharp depletion in the condensate due to three-body recombination. Naturally our two-body basis function will not be suitable to correctly describe the condensate in that situation. Such BEC dynamics can probably be successfully investigated using the number-conserving approach of Gardiner *et al.* [33].

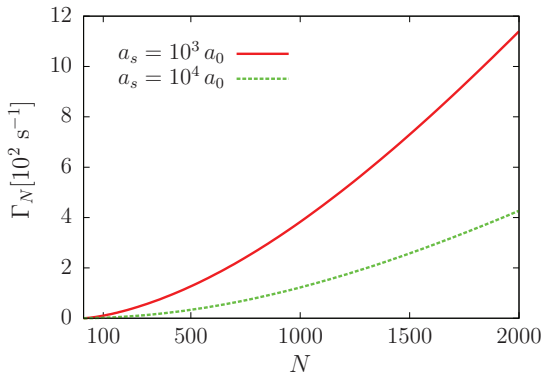


FIG. 7. (Color online) Plot of three-body loss rate $\Gamma_N$ as a function of $N$.

## IV. CONCLUSION

In this report we present the results of a quantum many-body calculation which keeps all possible two-body correlations to describe the interacting trapped Bose gas. Main attention has been paid in the deeper understanding of the effects of two-body correlations when the two-body interaction changes from a weak to a very strong one. In the first part of our work we investigate the properties when the $s$-wave scattering length is quite small ($na_s^3 \ll 1$). We have critically examined the limits of validity of SIA which is commonly used in the study of dilute BEC.

It is found that SIA is nicely obeyed when the number of bosons is less than 100. However, deviation occurs for larger $N$. As the previous calculations in this direction considered only few atoms, it is necessary to study the SIA for a large number of atoms and using a realistic potential instead of some model type of potentials. We also observe that the effect of interatomic correlation gradually builds in with an increase in $na_s^3$. Hence, our present study makes a correlation between the mean-field theory, which uses pure contact interaction, and the many-body theory, which uses realistic two-body interaction. We also apply our correlated basis function for large scattering length near the Feshbach resonance. We deliberately keep the number of atoms of the order of $10^4$ such that the condensate becomes strongly interacting but physically dilute and the application of a pair-correlated basis function is ideal for such a situation. The many-body results significantly differ from the mean-field results. Although the additional correction in the MGP retrieves the failure of GP in the intermediate scattering length, still this single correction is not enough for stronger interactions. Our study shows that an extra long-range shape-dependent correction term to the MGP is indeed necessary for very strongly interacting condensates.

We also calculate the monopole excitation frequency at large scattering length for finite $N$. Comparison with the beyond mean-field approximation strongly exhibits the role of the interatomic interaction. Finally, we observe the universal behavior in the interaction energy when the scattering length is quite large and comparable with trap size. Our many-body method can be extended for a large particle number limit easily.

As an extra advantage over the mean-field theory, our many-body calculation keeps all possible two-body correlations and considers both the beyond mean-field and finite-size effects.

Some related open questions are still there for future interest. As for very large scattering length and in the large particle number limit, the condensate becomes strongly correlated, and beyond two-body collisions may play a significant role. It indicates the importance of incorporating correlations beyond two-body ones for dense condensates. Our present calculation is limited to one side of the resonance, where $a_s$ is large positive and a strongly repulsive condensate is produced for any $N$. However, on the other side of the resonance (where scattering length is large negative), the condensate collapses for $N$ larger than a critical number. This will provide an interesting scenario of the collapse-growth cycle of ultracold clouds.

## ACKNOWLEDGMENT

B.C. and T.K.D. would like to thank the University of South Africa for financial assistance and hospitality during their visits to that University.

## APPENDIX A: RELATION OF THE EFFECTIVE RANGE TO SCATTERING LENGTH

In Fig. 8 we show $a_s$ as a function of $\ln(r_c)$ for the experimental value of $C_6 = 6.489\,75 \times 10^{-11}$ o.u. As $r_c$ decreases from a large value, $a_s$ decreases monotonically until it passes through an infinite discontinuity at a particular value of $r_c$ when the potential just supports a two-body bound state and $\eta(r_{ij})$ has a node. As $r_c$ is further decreased, $a_s$ decreases from a large positive value and the pattern repeats. One extra two-body bound state appears in each discontinuity. The hard core in the van der Waals potential is a model for the strong short-range repulsion. This will be valid when the average interparticle separation ($\sim N^{-1/3}$ o.u.) is much larger than $r_c$. It is indeed true for $N < 10^7$.

In Ref. [34], Fu *et al.* proposed the energy dependence of the scattering amplitude through an effective range expansion. For a hard-sphere potential the effective range ($r_e$) and the scattering length ($a_s$) maintains the relation $r_e = \frac{2}{3}a_s$. Thus $r_e$ increases essentially linearly with the scattering length. This does not match with the experimental condition where the scattering length is tuned by tuning the atomic resonance. The scattering length for a realistic van der Waals potential is related to the effective range $r_e$ by [35]

$$\frac{r_e}{\beta_6} = \left(\frac{2}{3x_e}\right)\frac{1}{(a_s/\beta_6)^2}\left\{1+\left[1-x_e\left(\frac{a_s}{\beta_6}\right)\right]^2\right\}, \quad \text{(A1)}$$

where $\beta_6 = (mC_6/\hbar^2)^{1/4}$ is the length scale of the van der Waals interaction and $x_e$ is a constant. For such an attractive long-range potential with a large $a_s$, the effective range almost does not change with tuning the scattering length. Therefore, with the van der Waals potential, a large positive scattering length can be achieved while maintaining the effective range.

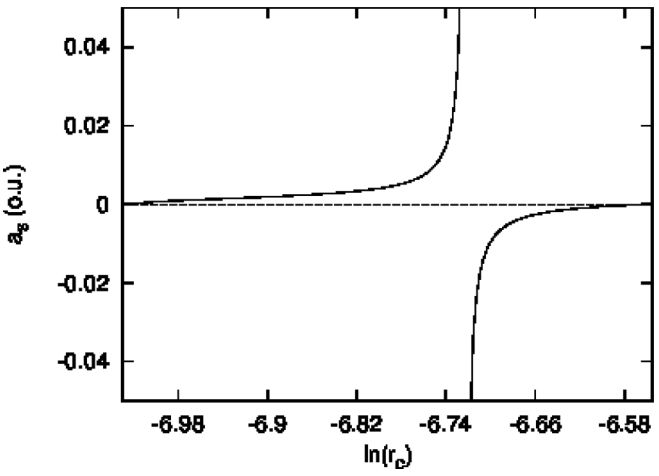


FIG. 8. Plot of scattering length ($a_s$) against $\ln(r_c)$.

## APPENDIX B: THE GP EQUATIONS

The mean-field time-independent GP equation for the ground-state wave function of the condensate is given by

$$\left[-\frac{\hbar^2}{2m}\nabla^2+\frac{1}{2}m\omega_{\rm ho}^2r^2+\frac{4\pi\hbar^2a_s'}{m}\left|\phi_{\rm GP}(\vec{r})\right|^2\right]\phi_{\rm GP}(\vec{r}) = \epsilon_{\rm GP}\phi_{\rm GP}(\vec{r}), \quad \text{(B1)}$$

where $\epsilon_{\rm GP}$ is the orbital energy and $\phi_{\rm GP}(\vec{r})$ is the ground-state orbital normalized to 1 and $a_s' = (N-1)\,a_s$. The total energy $E_{\rm GP}$ is obtained from the energy functional [9]. Note that GP energy depends on the product $(N-1)\,a_s$ rather than $a_s$ and $N$ separately. The quantity $(N-1)$ in the nonlinear term instead of $N$ comes from the number conserving Schrödinger quantum mechanics [36].

While the GP equation considers only the mean-field interaction which comes from the nonlinear term in Eq. (B1), the MGP equation contains beyond-mean-field quantum correction. The correction to the mean-field equation was included by Braaten and Nieto [13] which takes the effect of quantum fluctuation into account. In the Thomas-Fermi (TF) approximation the quantum correction adds an additional local term in the mean-field effective potential in the GP equation as

$$\left[-\frac{\hbar^2}{2m}\nabla^2+\frac{1}{2}m\omega_{\rm ho}^2r^2+\frac{4\pi\hbar^2a_s'}{m}|\phi_{\rm MGP}(\vec{r})|^2 \times\left(1+\frac{32(a_s')^{3/2}}{3\sqrt{\pi}(N-1)}|\phi_{\rm MGP}(\vec{r})|\right)\right]\phi_{\rm MGP}(\vec{r}) = \epsilon_{\rm MGP}\phi_{\rm MGP}(\vec{r}), \quad \text{(B2)}$$

where the total energy $E_{\rm MGP}$ can be obtained from the energy functional. Note that the GP equation depends only on the total interaction parameter $(N-1)\,a_s$, whereas Eq. (B2) depends separately on $(N-1)$ and $a_s$. Thus Eq. (B2) accounts for two-body physics. Although the MGP equation includes some effects due to correlations, it is still independent of the shape of the interatomic potential.

[1] C. C. Bradley, C. A. Sackett, J. J. Tollett, and R. G. Hulet, Phys. Rev. Lett. **75**, 1687 (1995).
[2] J. L. Roberts, N. R. Claussen, S. L. Cornish, E. A. Donley, E. A. Cornell, and C. E. Wieman, Phys. Rev. Lett. **86**, 4211 (2001).
[3] S. L. Cornish, N. R. Claussen, J. L. Roberts, E. A. Cornell, and C. E. Wieman, Phys. Rev. Lett. **85**, 1795 (2000).
[4] E. A. Donley, N. R. Claussen, S. L. Cornish, J. L. Roberts, E. A. Cornell, and C. E. Wieman, Nature (London) **412**, 295 (2001).
[5] S. B. Papp, J. M. Pino, R. J. Wild, S. Ronen, C. E. Wieman, D. S. Jin, and E. A. Cornell, Phys. Rev. Lett. **101**, 135301 (2008).
[6] N. R. Claussen, E. A. Donley, S. T. Thompson, and C. E. Wieman, Phys. Rev. Lett. **89**, 010401 (2002).
[7] S. E. Pollack, D. Dries, M. Junker, Y. P. Chen, T. A. Corcovilos, and R. G. Hulet, Phys. Rev. Lett. **102**, 090402 (2009).
[8] M. H. Anderson, J. R. Ensher, M. R. Matthews, C. E. Wieman, and E. A. Cornell, Science **269**, 198 (1995).
[9] F. Dalfovo, S. Giorgini, L. P. Pitaevskii, and S. Stringari, Rev. Mod. Phys. **71**, 463 (1999).
[10] S. Cowell, H. Heiselberg, I. E. Mazets, J. Morales, V. R. Pandharipande, and C. J. Pethick, Phys. Rev. Lett. **88**, 210403 (2002).
[11] J. L. Bohn, B. D. Esry, and C. H. Greene, Phys. Rev A **58**, 584 (1998).
[12] D. Blume and C. H. Greene, Phys. Rev. A **63**, 063601 (2001).
[13] E. Braaten and A. Nieto, Phys. Rev. B **56**, 14745 (1997).
[14] E. Timmermans, P. Tommasini, and K. Huang, Phys. Rev. A **55**, 3645 (1997).
[15] A. Fabrocini and A. Polls, Phys. Rev. A **60**, 2319 (1999).
[16] S. Geltman, Chem. Phys. Lett. **418**, 163 (2006); Phys. Lett. A **356**, 431 (2006); Mol. Phys. **106**, 1369 (2008).
[17] S. Giorgini, J. Boronat, and J. Casulleras, Phys. Rev. A **60**, 5129 (1999).
[18] I. Khan and B. Gao, Phys. Rev. A **73**, 063619 (2006); B. Gao, J. Phys. B **37**, L227 (2004).
[19] E. Braaten, H.-W. Hammer, and T. Mehen, Phys. Rev. Lett. **88**, 040401 (2002).
[20] J. L. Song and F. Zhou, Phys. Rev. Lett. **103**, 025302 (2009).
[21] B. A. McKinney, M. Dunn, and D. K. Watson, Phys. Rev. A **69**, 053611 (2004).
[22] M. Thogersen, D. V. Fedorov, and A. S. Jensen, Europhys. Lett. **79**, 40002 (2007).
[23] S. A. Sofianos, T. K. Das, B. Chakrabarti, M. L. Lekala, R. M. Adam, and G. J. Rampho, Phys. Rev. A **87**, 013608 (2013).
[24] T. K. Das and B. Chakrabarti, Phys. Rev. A **70**, 063601 (2004).
[25] J. L. Ballot and M. Fabre de la Ripelle, Ann. Phys. (NY) **127**, 62 (1980).
[26] M. Fabre de la Ripelle, Ann. Phys. (NY) **147**, 281 (1983).
[27] T. K. Das, S. Canuto, A. Kundu, and B. Chakrabarti, Phys. Rev. A **75**, 042705 (2007).
[28] T. K. Das, A. Kundu, S. Canuto, and B. Chakrabarti, Phys. Lett. A **373**, 258 (2009).
[29] C. J. Pethik and H. Smith, *Bose-Einstein Condensation in Dilute Gases* (Cambridge University Press, Cambridge, England, 2001).
[30] T. K. Das, H. T. Coelho, and M. Fabre de la Ripelle, Phys. Rev. C **26**, 2281 (1982).
[31] R. P. Tiwari and A. Shukla, Comput. Phys. Commun. **174**, 966 (2006).
[32] L. Pitaevskii and S. Stringari, Phys. Rev. Lett. **81**, 4541 (1998).
[33] S. A. Gardiner and S. A. Morgan, Phys. Rev. A **75**, 043621 (2007).
[34] H. Fu, Y. Wang, and B. Gao, Phys. Rev A **67**, 053612 (2003).
[35] B. Gao, Phys. Rev. A **58**, 4222 (1998).
[36] B. D. Esry, Phys. Rev. A **55**, 1147 (1997).